

Diacylglycerol transport in the insect fat body: evidence of involvement of lipid droplets and the cytosolic fraction

Estela L. Arrese,^{1,†} Justin L. Gazard,* Matthew T. Flowers,* Jose L. Soulages,[†] and Michael A. Wells*

Department of Biochemistry and Center for Insect Science,* University of Arizona, Tucson, AZ 85721; and Department of Biochemistry and Molecular Biology,[†] 246 Noble Research Center, Oklahoma State University, Stillwater, OK 74078

Abstract In this report we show the existence of a distinct pool of fat body diacylglycerol (DG) that can be distinguished from the bulk DG. This is a dynamic pool of DG that uses FA entering the fat body from the hemolymph, whereas the bulk DG uses the fatty acids stored in the fat body fat droplets. Using a dual labeling technique, it was possible to compare the effect of hormone-stimulated DG synthesis and secretion on the distribution of radiolabeled FA among the lipids of the dynamic pool (short-term radiolabeling), with the hormonal effect on the total complement of fat body lipids (long-term radiolabeling). We observed that, whereas DG represents 2% to 3% of the fat body lipid mass, about 20% of the short-term radiolabeled lipids are represented by DG. Stimulation of lipolysis produces a fast decrease in the fraction of short-term radiolabeled DG, whereas there is an increase in the mass of fat body DG. The subcellular distribution of bulk DG showed that its majority (62%) was in the fat cake whereas only 2.9% was in the cytosol. On lipolysis stimulation, the largest changes in specific activities of newly synthesized DG were detected in the cytosol and the fat cake, suggesting that newly synthesized DG localized in the lipid droplets and the cytosol is preferentially mobilized.—Arrese, E. L., J. L. Gazard, M. T. Flowers, J. L. Soulages, and M. A. Wells. **Diacylglycerol transport in the insect fat body: evidence of involvement of lipid droplets and the cytosolic fraction.** *J. Lipid Res.* 2001. 42: 225–234.

Supplementary key words AKH • *Manduca sexta* • lipolysis • lipid mobilization

Many insects such as *Manduca sexta*, which rely on lipids as the major fuel for flight, mobilize *sn*-1,2-diacylglycerol (DG) into the circulation (1, 2). DG is derived from triacylglycerol (TG) stores in the fat body and constitutes the main form in which FA (FA) are mobilized to the site of utilization, for example, flight muscle. Mobilization of lipid stores is signaled by the release of a nonapeptide, adipokinetic hormone (AKH), from the cephalic region (3). We have shown in the *M. sexta* fat body that AKH rapidly

activates a cAMP-dependent protein kinase (4) as well as the phosphorylatable TG lipase (5). Because the kinase activation precedes the activation of the lipase, which in turn precedes the appearance of DG in circulation, the stimulation of lipolysis induced by AKH might be regulated by phosphorylation reactions. In vertebrates, the mechanisms of action of lipolytic hormones on fat cells are believed to be mediated by the cAMP-dependent activation of hormone-sensitive lipase [reviewed in refs. (6 and 7)]. However, new evidence suggesting that the lipolytic hormone acts on the endogenous lipid substrate rather than on the lipase has been reported (8, 9). In addition, we have also indicated that stored TG is the direct precursor of the DG that is released from the fat body (2, 10). In other words, direct stereospecific hydrolysis of TG catalyzed by the TG lipase is the pathway for the synthesis of DGs that are released into the hemolymph.

In the circulation, DG is transported by lipophorin, the major insect lipoprotein (1, 11). A characteristic feature of insect lipophorin is that it acts as a reusable lipid shuttle. The turnover of DG occurs at a much higher rate than that of the protein component of lipophorin (12). Lipophorin can load and unload lipid without internalization of the lipoprotein. DG is transferred into preexisting high density lipophorin at the surface of the fat body by a mechanism that is facilitated by lipid transfer particle, but that remains to be elucidated (13). As the DG content of lipophorin increases, there is a concomitant association of apolipoprotein III with these particles (11). The resulting larger and less dense low density lipophorin has a greater capacity to transport DG from the fat body to the flight

Abbreviations: AKH, adipokinetic hormone; DG, diacylglycerol; FFA, free FA; MG, monoacylglycerol; PL, phospholipids; TG, triacylglycerol; TLC, thin-layer chromatography

¹ To whom correspondence should be addressed.

e-mail: estela@biochem.okstate.edu

muscle. The transport of DG by lipophorin has been the focus of extensive studies. However, there is no information about the intracellular transport of DG or the mechanism by which DG is released from the intracellular compartment to the hemolymph.

As in vertebrate adipose tissue, TG is stored in the fat body cell in cytoplasmic droplets (14). The intracellular location of the fat body TG lipase seems to be the cytosol, from where this enzyme has been purified (15). The sequence of events leading to the activation of lipolysis could involve the translocation of the lipase to its substrate, which is present in the fat droplets. After the stimulation of lipid mobilization, the content of DG in the fat body gradually increases and simultaneously an enormous mobilization of DG into the hemolymph is observed (2).

As a part of our investigation of lipolysis in insects, we are interested in examining the mechanism by which DG is transported in the cell from the lipid droplets to the cell surface. This information is required to achieve a complete description of the lipolytic process that takes place in the insect fat body. In this article we show the occurrence of a distinct pool of fat body DG that can be distinguished from the bulk DG in the fat body. This is a dynamic pool of DG that uses FA entering the fat body from the hemolymph whereas the bulk DG uses the FA stored in the fat droplets. We also report an investigation of the intracellular location of bulk and newly synthesized DG (formed from FA injected in the hemolymph), as well as the effect of the lipolytic hormone AKH on that distribution. We have found that the newly synthesized DG localized in the fat cake and particularly in the cytosol are preferentially mobilized when lipid mobilization was stimulated by AKH. No change was observed in the DG localized in the particulate fraction. We conclude that newly synthesized DG pool could be used for studying the transport of DG within the cell. This information provides a starting point for future studies, which will focus on the characterization of the cytosolic components that are involved in intracellular DG transport.

MATERIALS AND METHODS

Materials

[2-¹⁴C]acetate was purchased from American Radiolabeled Chemicals (St. Louis, MO) and [9,10-³H]palmitic acid and [9,10(*n*)-³H]oleic acid were purchased from New England Nuclear (Boston, MA). *Manduca sexta* AKH was purchased from Peninsula Laboratories (Belmont, CA). Silica gel G plates were obtained from J. T. Baker (Phillipsburg, NJ) and Ficoll 400 from Amersham-Pharmacia (Piscataway, NJ). All other chemicals were of analytical grade.

Experimental insects

Two- or three-day old *M. sexta* adults from a colony maintained in the authors' laboratory were used (4). Adults were kept at 25°C without food. Animals were decapitated 24 h prior to being used. Before use, the decapitated insects were injected with 13 mg of trehalose dissolved in 20 μl of H₂O (5). After an additional 2 h, the insects were used for experiments. Typically, the lipid content of fat body and hemolymph is 84.6 ± 8.6 mg of

lipid per fat body and 12.9 ± 1.1 mg of lipid per insect, respectively (16). The following amounts of TG, DG, monoacylglycerol (MG), and free fatty acids (FFA) are found in the fat body: 82.70, 1.69, 0.05, and 0.18 mg per fat body, respectively; whereas the amounts of TG, DG, MG, and FFA in the hemolymph are 0.44, 12.30, 0.08, and 0.015 mg per insect, respectively (2).

Radiolabeling of fat body lipids

Fat body lipids were radiolabeled according to two different procedures: long and short term, respectively. A third procedure, which is a combination of these two, was used to produce dual-radiolabeled lipids.

Long-term procedure. Fat body lipids were radiolabeled following the long-term procedure previously reported (2). Briefly, during the fifth larval instar, insects were fed 20 μCi of [9,10-³H]-palmitic acid. After completion of development (32 days), radioactively labeled adults, 2 or 3 days after emergence, were decapitated and injected with trehalose as indicated above. After an additional 2 h, insects were injected with 100 pmol of AKH. Fat bodies were taken out 60 min after the hormone injection and used for lipid extraction.

Short-term procedure. Experimental insects were injected with 20 μCi of either [9,10(*n*)-³H]oleic acid or [9,10-³H]palmitic acid. Fat body was taken out at various times from 5 min up to 6 h, and subjected to lipid extraction. For the time point corresponding to 240 min both the fat body and hemolymph were collected and used for lipid analysis.

Dual radiolabeling of fat body lipids. During the fifth larval instar, insects were fed 20 μCi of [2-¹⁴C]acetate. After completion of development, adults were decapitated and subjected to short-term labeling by injection of 20 μCi of [9,10-³H]palmitic acid as indicated above. After 240 min, insects were injected with 100 pmol of AKH. Fat bodies were taken out at various times after the hormone injection and used for lipid extraction.

Sample preparation and lipid extraction

Individual fat body was dissected and lipids were extracted with chloroform-methanol (17). A small aliquot (50 μl) of the lipid extract was used for determination of the total lipid radioactivity by liquid scintillation counting.

Lipid separation

The lipids in the extracts were separated by thin-layer chromatography (TLC) on silica gel G plates, using hexane-ethyl ether-formic acid 70:30:3 (v/v/v) as the developing solvent. The MG, DG, FFA, and TG fractions, along with material that remained at the origin, the phospholipid fraction (PL), were visualized with I₂ vapor and scraped from the plate, and the radioactivity was counted by liquid scintillation counting. The same efficiency of counting was obtained for all the samples. Results were expressed as a percentage of total radioactivity (mean ± SEM, n value as indicated below).

Distribution of radiolabel between the glycerol backbone and FA in acylglycerols

TLC-separated TG and DG from dual-radiolabeled insects were scraped from the plate and lipids were eluted from the silica gel with diethyl ether (18) and concentrated to dryness under a stream of nitrogen. The distribution of radiolabel between the backbone and the fatty acyl chains was analyzed as previously reported (2).

Positional distribution of radiolabeled FA in acylglycerols

TLC-separated TG and DG from dual-radiolabeled insects were scraped from the plate as indicated above and concen-

trated to dryness under a stream of nitrogen. Lipid samples were used to analyze the positional distribution of the radioactively labeled FA according to Arrese and Wells (2) and Brockman (19).

Fat body subcellular fractionation

The fractionation was carried out according to the procedure described for the subcellular fractionation of adipocytes (20). Fat bodies obtained under the following conditions were subjected to the subcellular fractionation: *a*) long-term radiolabeling; *b*) long-term radiolabeling, AKH injected; *c*) short-term radiolabeling; and *d*) short-term radiolabeling, AKH injected. In all cases, lipids were radiolabeled by using 20 μCi of [^3H]palmitic acid per insect as indicated above.

Fat bodies dissected from 20 insects were pooled and homogenized at 3,000 rpm with a Potter-Elvehjem glass homogenizer fitted with a Teflon pestle, using 20 ml of buffer A [10 mM Tris, 1 mM ethylenediaminetetraacetic acid (EDTA), 250 mM sucrose, 0.1% (v/v) 2-mercaptoethanol, 0.05% (v/v) diisopropyl fluorophosphate, pH 7.4]. The resulting homogenate was placed in ice, and all subsequent steps were carried out at 4°C. The homogenate was centrifuged (1,000 *g* for 10 min) to pellet unbroken cells, cell debris, and nuclei, which were discarded. The resulting supernatant (fraction 0) was centrifuged (20,000 *g* for 25 min) and three different fractions were collected: fat cake, infranatant, and 20,000 *g* pellet. The fat cake containing the store lipid droplets (fraction 1) was collected into a separate glass tube. The infranatant containing the microsomes and cytosol was recentrifuged at 160,000 *g* for 80 min, yielding a supernatant (fraction 2, cytosol) and a pellet (fraction 4, microsomal fraction).

The 20,000 *g* pellet (fraction 3, plasma membranes and mitochondria) was resuspended in 8 ml of buffer A and placed on a discontinuous Ficoll gradient. This gradient consisted of two 10-ml Ficoll layers, 15% (bottom) and 9% (top), respectively. After centrifugation (21,200 rpm for 45 min) in an SW27 rotor, the Ficoll gradient fractionation yielded two distinct fractions: the plasma membrane fraction (3-a) that formed a band on top of the 9% layer and the mitochondria that were collected in the pellet (fraction 3-b).

An aliquot of the cytosolic fraction was subjected to KBr density gradient separation. For this purpose, 7.2 g of KBr was dissolved in 16 ml of supernatant. This preparation was overlaid with 23 ml of buffer [100 mM Na_2HPO_4 , 150 mM NaCl, 2 mM EDTA, 0.002% (w/v) Na_3N , pH 6.5]. After centrifugation (50,000 rpm for 16 h) in a VTi50 vertical rotor, the gradient was fractionated from top to bottom into 1-ml fractions and the optical density at 280 nm and radioactivity were determined. Radioactivity was counted in 100- μl aliquots by liquid scintillation counting. Fractions 1–9, 10–18, 19–27, and 28–36 were pooled. The density of each pool was measured. Pools were used for protein assays and lipid extracts.

The following determinations were carried out in each subcellular fraction: *a*) total radioactivity, and *b*) distribution of radioactivity among the lipids. Total radioactivity was determined by counting an aliquot of each subcellular fraction, using liquid scintillation counting. Results are expressed as percentage: [cpm recovered in the subcellular fraction/cpm recovered from the fat body homogenate (0)] \times 100. Distribution of radioactivity among the lipids was determined by TLC as indicated above. Results are expressed as a percentage of the counts per minute, where the sum of counts per min obtained for TG, DG, FFA, MG, and PL in each subcellular fraction represents 100%.

The percentage of DG in each subcellular fraction (y_1) was expressed as a percentage of total counts per min: [(% of DG in fraction y_1) \times (% of total radioactivity of fraction y_1)]/100.

Other procedures

Protein concentration was determined by the Bradford dye-binding assay, using bovine serum albumin as a standard (21).

Statistics

Results are presented as means \pm SEM. Statistical comparisons were made by the Student's *t*-test; $P < 0.05$ was considered to be significant.

RESULTS

Newly synthesized fat body lipids

TG comprised the main fat body lipid, making up 94.3% of total lipid mass (2). The FA composition of TG indicated that palmitic acid (16:0), oleic acid (18:1), and linoleic acid (18:2) were the prevalent FA, comprising 28.2 ± 1.1 , 31.6 ± 0.6 , and 29.2 ± 0.8 mol%, respectively (E. L. Arrese and M. A. Wells, unpublished results). The remaining fat body lipids were DG, MG, FFA, and PL, which accounted for 2.6%, 0.2%, 0.5%, and 2.3% of the total lipid mass, respectively (2).

To determine the composition of recently synthesized fat body lipids, experimental insects were injected with 20 μCi of [^3H]palmitic acid (16:0). At different times, fat body lipid extracts were analyzed for distribution of radioactivity as indicated in Materials and Methods. **Figure 1A** shows the class composition of lipid radioactivity. Within 4 h the proportion of radioactive TG increased up to 70%. PL and MG did not accumulate a significant proportion of label, which represented about 4% and 0.5%, respectively. However, a notable accumulation of radioactivity as DG was found. Within 30 min the proportion of radioactive DG leveled off at about 21% and remained nearly constant for 5 h.

Figure 1B shows the class composition of lipid radioactivity after the injection of 20 μCi of [^3H]oleic acid (18:1). As indicated above, oleic acid was also a relevant FA of the insect fat body, comprising about 32% of the total content of FA. The conversion of [^3H]oleic acid into lipids was somewhat faster than in the case of [^3H]palmitic acid. For example, 2 h after the injection, the radiolabeled FFA represented about 4% of the radiolabeled lipids instead of the 20% detected in the case of [^3H]palmitic acid (Fig. 1A). A similar proportion of newly synthesized TG that reached 70% within 3 h was also observed. In the case of PL, a slightly higher proportion of PL (10% to 11%) was observed at earlier time points, but then this value decreased, remaining constant at about 5%. Similar to the incorporation of [^3H]palmitic acid, a small fraction of the label was found as MG. Likewise, a high accumulation of [^3H]DG was also detected. Within 15 min after the injection of [^3H]palmitic acid, the radioactivity found as DG rapidly increased to 23% of total radioactive lipids and remained constant during the course of the experiment.

The patterns of the distribution of radioactivity among newly synthesized lipids obtained from labeled palmitic acid and oleic acid were generally similar, with certain differences observed over short periods of time. In these experiments, a significant difference between the distribu-

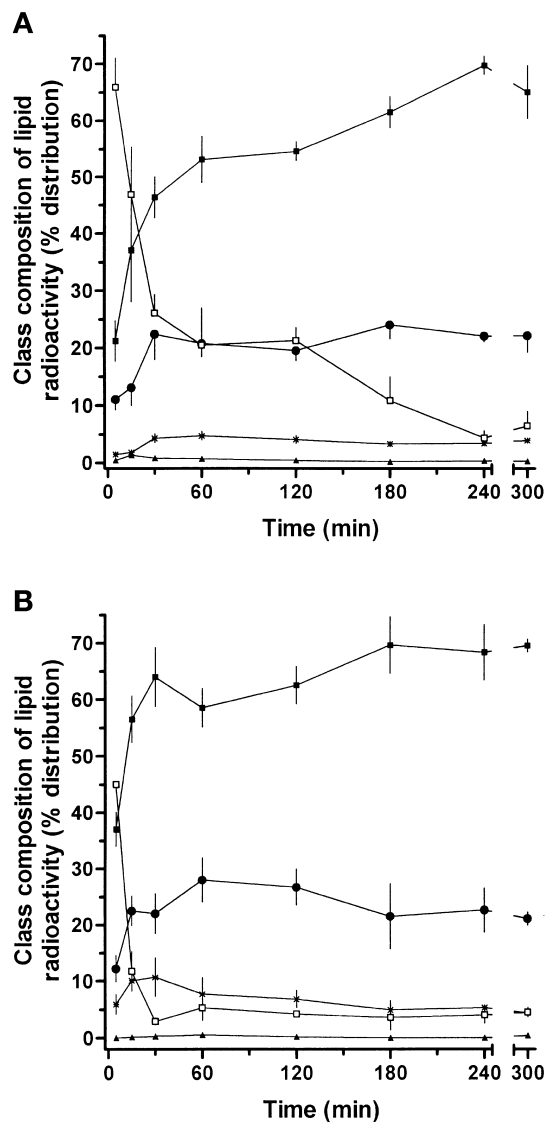


Fig. 1. A: Class composition of lipid radioactivity (% distribution) after the injection of 20 μCi of [^3H]palmitic acid. Fat body lipid extracts were separated by TLC. The distribution of radioactivity was determined by liquid scintillation counting of silica gel scrapings. Results are expressed as a percentage of total counts per min \pm SEM ($n = 6$), where the sum of counts per min obtained from TG (solid squares), DG (solid circles), FFA (open squares), PL (asterisks), and MG (solid triangles) represents 100%. Total counts per min recovered from the fat body of one insect was $4.6 (\pm 0.7) \times 10^6$. B: Class composition of lipid radioactivity (% distribution) after the injection of 20 μCi of [^3H]oleic acid. Fat body lipid extracts were separated by TLC. The distribution of radioactivity was determined by liquid scintillation counting of silica gel scrapings. Results are expressed as a percentage of total counts per min \pm SEM ($n = 6$), where the sum of counts per minute obtained from TG (solid squares), DG (solid circles), FFA (open squares), PL (asterisks), and MG (solid triangles) represents 100%. Total counts per min recovered from the fat body of one insect was $8.9 (\pm 1.7) \times 10^6$.

tion of radioactivity among newly synthesized lipids and the distribution of mass of fat body lipids was found. As can be seen in Fig. 1, with both labeled oleic and palmitic acid, about 20% of the lipid radioactivity was in DG. Because less than 3% of the mass of total fat body lipids is

DG (Materials and Methods) the accumulation of radioactivity in newly synthesized DG indicates that this lipid formed a separated pool in the fat body cell. This pool does not equilibrate rapidly with the TG pool because, at least 5 h after the incorporation of radioactive FA, the proportion of newly synthesized DG remained unchanged, representing about 20% of total radioactive lipids.

Preliminary results on the effect of AKH on newly synthesized fat body DG showed that AKH induced a pronounced decrease in the [^3H]DG of the fat body. The percentage of total radioactivity found in newly synthesized fat body DG after the stimulation of lipolysis by AKH decreased to 7.9% and 11.2% in the insects labeled with [^3H]oleic acid and [^3H]palmitic acid, respectively. Because we know that AKH induces an accumulation of DG in both the hemolymph and the fat body (2), this result was clearly unexpected. To investigate further the nature of the AKH-induced changes in the composition of recently synthesized lipids, particularly DG, we decided to investigate this effect with insects in which the bulk lipids were distinguishable from the newly synthesized lipids.

Effect of AKH on bulk and newly synthesized DG by using dual-radiolabeled fat body lipids

Dual-radiolabeled fat body lipids were obtained after a long- and short-term radiolabeling procedure with the same group of insects, using [^{14}C]acetate and [^3H]palmitic acid for the long- and short-term procedures, respectively. Thus, bulk lipids were radiolabeled with ^{14}C and newly synthesized lipids were radiolabeled with ^3H . Analysis of the distribution of the radiolabel in the TG molecule showed that 98% of the radioactivity associated with ^{14}C was in the FA and 2% was in the glycerol backbone. Similarly, 99% of the radioactivity associated with ^3H was in the FA. Analysis of the positional distribution of radiolabeled FA in the fat body TG indicated that 90% of ^{14}C -labeled FA and 87% of ^3H -labeled FA were incorporated into the *sn*-1(3) position, whereas 10% and 13%, respectively, were in the *sn*-2 position.

Using [^3H]oleic acid and [^3H]glycerol, we have previously shown that the long-term (32 days) radiolabeling procedure leads to a homogeneous distribution of radiolabel in the lipid species in the fat body (2). The distribution of radioactivity among the acylglycerols is equivalent to the content of acylglycerols in both the fat body and hemolymph. Therefore, by using a different isotope to obtain the short-term radiolabeling, it is possible to have insects in which both bulk and newly synthesized lipids are distinguishable.

Table 1 shows the distribution of radioactivity among the fat body lipid classes before AKH injection in dual-labeled insects. As expected, the distribution of ^{14}C -labeled (bulk) lipids reflected the relative mass of the lipid species in the fat body, whereas ^3H -labeled (newly synthesized) lipids showed a relative excess of label in DG. The specific activities of [^{14}C]DG and [^3H]DG were $0.71 \times 10^5 \pm 0.02 \times 10^5$ cpm/mg and $1.21 \times 10^6 \pm 0.04 \times 10^6$ cpm/mg, respectively.

Figure 2 shows the time course of the changes of radioactive fat body DG after the injection of AKH into dual-

TABLE 1. Class composition of lipid radioactivity of dual-radiolabeled insects

	Lipid Class (%)				
	TG	DG	MG	FFA	PL
¹⁴ C-labeled lipids (long-term; n = 6)	95.45 ± 0.35	2.45 ± 0.09	0.08 ± 0.10	0.51 ± 0.19	1.47 ± 0.27
³ H-labeled lipids (short-term; n = 6)	60.73 ± 2.26	22.52 ± 1.51	0.40 ± 0.15	8.03 ± 2.27	7.46 ± 1.21

Insects were fed [¹⁴C]acetic acid at the larval stage, and after 32 days insects at the adult stage were injected with [³H]palmitic acid. Fat body lipid extracts were analyzed by TLC as indicated. Results are expressed as a percentage of the counts per min, where the sum of the total classes of lipids (PL, MG, DG, FFA, and TG) for each isotope represents 100%. The total counts per min recovered from the fat body of one insect was $4.9 \times 10^6 \pm 0.7 \times 10^6$ as ¹⁴C-labeled lipids and $9.1 \times 10^6 \pm 1.1 \times 10^6$ as ³H-labeled lipids. Values represent means ± SEM of n experiments.

labeled insects. A gradual increase in the level of [¹⁴C]DG, which was significant after 60 min ($P = 0.003$), was observed. The proportion of radioactivity as [¹⁴C]DG increased from 2.5% to 4.5% in that period of time. Previously, we have shown that AKH-induced lipolysis produces an accumulation of DG in the fat body (2). As in previous experiments, the levels of FFA, MG, and PL remained nearly constant during the progress of the experiment (data not shown).

However, AKH treatment exhibited an opposite effect on newly synthesized [³H]DG, eliciting a significant decrease in the proportion of [³H]DG (Fig. 2). [³H]DG de-

creased from 22.5% to 12.1% 1 h after AKH injection. This result confirmed our preliminary observations of the effect on the newly synthesized fat body DG obtained with [³H]oleic acid and [³H]palmitic acid (see above). The specific activity of [¹⁴C]DG and [³H]DG after 60 min of induction of lipid mobilization was 0.70×10^5 and 0.35×10^6 cpm/mg, respectively. Therefore a 3.4-fold decay was obtained in the specific activity of [³H]DG, whereas the variation in the specific activity [¹⁴C]DG was not significant.

In the hemolymph, after 1 h of stimulation of lipolysis by AKH, the mass of DG increased from 12.3 to 21.4 mg per insect. The specific activity of hemolymph [³H]DG was $0.39 \times 10^6 \pm 0.1 \times 10^6$ cpm/mg before the AKH treatment (0 min) and $0.29 \times 10^6 \pm 0.08 \times 10^6$ cpm/mg after the AKH injection (60 min), showing that a 1.3-fold decrease in [³H]DG was observed. The change in specific activity being smaller than the change in mass (1.7-fold) supports the notion that [³H]DG was mobilized to the hemolymph. Moreover, the specific activity of hemolymph [¹⁴C]DG was $0.41 \times 10^5 \pm 0.04 \times 10^5$ cpm/mg and $0.54 \times 10^5 \pm 0.02 \times 10^5$ cpm/mg before (0 min) and after (60 min) the stimulation of lipolysis by AKH, respectively. These results are consistent with the fact that both [³H]DG and [¹⁴C]DG were secreted from the fat body to the hemolymph.

Subcellular distribution of newly synthesized and bulk DG

We investigated the subcellular localization of fat body DG (newly synthesized and bulk) in resting insects as well as in insects in which lipolysis was stimulated by AKH. The distribution of newly synthesized lipids (short term) among the major subcellular components was investigated in experimental insects that were injected with 20 μ Ci of [³H]palmitic acid. Four hours later, half the insects were treated with 100 pmol of AKH. After an additional 1 h, fat bodies were dissected and used for the subcellular fractionation as indicated in Materials and Methods. Likewise, the same studies were carried out with insects whose fat body lipids were long-term radiolabeled (bulk) by feeding 20 μ Ci of [³H]palmitic acid at the larval stage. Half these insects, in which the bulk lipids were radiolabeled, were also treated with AKH and fat bodies used for subcellular fractionation.

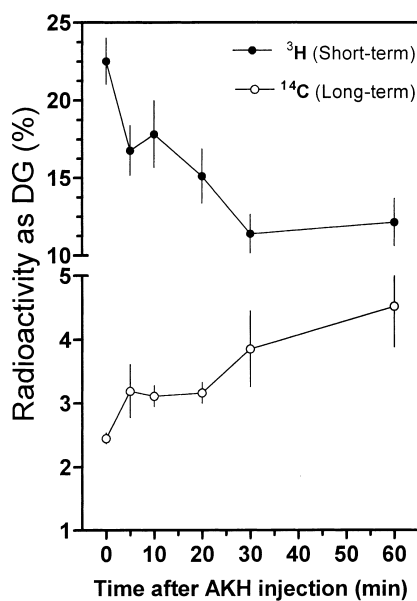


Fig. 2. Time course of the distribution of fat body radioactive DG after the injection of AKH in insects in which the fat body lipids were dual radiolabeled as indicated in Materials and Methods. Fat body lipid extracts were separated by TLC. The distribution of radioactivity was determined by liquid scintillation assay of silica gel scrapings. Results are expressed as a percentage of total counts per min ± SEM (n = 6), where the sum of counts per min obtained from PL, MG, DG, FFA, and TG for each isotope, individually, represents 100%. Total counts per min recovered from the fat body of one insect after 60 min of AKH injection was 8.1 ± 1.7 of ³H-labeled lipids and $4.4 (\pm 0.7) \times 10^6$ of ¹⁴C-labeled lipids.

TABLE 2. Distribution of radioactivity among fat body lipid classes in whole homogenate from insects that were short-term (newly synthesized) or long-term (bulk) radiolabeled with [³H]palmitic acid

	Lipid Class (%)				
	TG	DG	MG	FFA	PL
Short-term (n = 4)	53.60 ± 6.30	22.10 ± 3.50	1.09 ± 0.46	17.50 ± 5.90	5.70 ± 2.15
Long-term (n = 3)	93.04 ± 1.24	3.25 ± 0.27	0.45 ± 0.23	1.83 ± 0.33	1.48 ± 0.77
Short-term /AKH (n = 3)	72.70 ± 3.50	10.80 ± 0.18	0.76 ± 0.22	13.23 ± 2.11	3.93 ± 0.56
Long-term /AKH (n = 4)	91.40 ± 0.42	5.11 ± 0.32	0.51 ± 0.26	1.88 ± 0.31	1.10 ± 0.16

Similar insects also were treated with AKH, respectively. Results are expressed as a percentage of the counts per min, where the sum of classes of lipids (PL, MG, DG, FFA, and TG) represent 100%. The total counts per min recovered from the fat body of one insect was $8.4 (\pm 1.4) \times 10^6$, $6.2 (\pm 1.2) \times 10^6$, $6.3 (\pm 0.9) \times 10^6$, and $5.6 (\pm 0.8) \times 10^6$ for short term, long term, short term/AKH, and long term/AKH, respectively. Values represent means ± SEM of n experiments.

Table 2 shows the distribution of radioactivity among fat body lipid classes in whole fat body homogenate before performing the subcellular fractionation. In agreement with the previous results, the distribution of radioactivity among the newly synthesized lipids differed from the distribution of radioactivity among the bulk lipids. Newly synthesized lipids exhibited higher proportions of DG and FFA (Table 2). Thus, the distribution of radioactivity obtained in this case is consistent with the values obtained with the dual-labeled insects (Table 1 and Fig. 2).

Table 3 shows the distribution of total radioactivity among the four major subcellular components. Results obtained with long-term radiolabeling indicate that the vast majority of the bulk lipids (90.7%) is found in the fat cake, whereas the cytosol contains the smallest portion (0.9%) of total lipids. The distribution of total radioactivity in the case of newly synthesized lipids differs from the distribution of radioactive bulk lipids. The portion of total radioactive lipids in the fat cake is much lower (62.8%), with a concomitant increase in total radioactive lipids in the remaining fractions (Table 3).

TLC determination of the distribution of radioactivity among the lipid classes in each subcellular fraction (data not shown) combined with the distribution of total radioactivity among subcellular fractions (Table 3) permits calculation of the fraction of each lipid class present in each subcellular fraction. **Table 4** shows the distribution of DG

among the four major subcellular components. In resting insects, the majority (62%) of bulk DG was located in the fat cake fraction, whereas 3% of the DG was found in cytosol. The remaining radioactive DG distributed between the low and high speed pellets. The former contains the plasma membranes and mitochondrial fractions and the latter is the microsomal fraction (16). After AKH stimulation, the proportion of DG in the whole fat body increased from 3.21% to 5.47% (Table 4). This increased DG was found only in the fat cake and the cytosol. The fat cake DG increased 2.4-fold, whereas a 3.4-fold increase was found in the cytosol.

On the other hand, newly synthesized DG under resting conditions distributed as follows: 58% in the fat cake, 33% between the low and high speed pellets, and 9% in the cytosolic fraction (Table 4). After AKH treatment, the accumulation of radioactivity in newly synthesized DG in the fat body declined from 21.6% to 10.2% and all four subcellular fractions exhibited a lower proportion of newly synthesized DG (Table 4). Among them, the cytosolic and microsomal fractions were the two fractions in which AKH produced the biggest decrease in DG proportion. As a control for the fractionation procedure, Table 4 shows that the sum of the percentage of DG in each subcellular fraction was similar to values obtained with the whole homogenate, proving that the fractionation did not produce any significant loss of material.

TABLE 3. Distribution of total radioactivity among the subcellular fractions from insects that were short-term or long-term radiolabeled with [³H]palmitic acid

Subcellular Fraction	Total Radioactivity (%)			
	Long Term		Short Term	
	-AKH (n = 3)	+AKH (n = 4)	-AKH (n = 4)	+AKH (n = 3)
Fat cake (1)	90.73 ± 3.38	92.68 ± 2.11	62.85 ± 8.30	77.60 ± 0.94
Cytosol (2)	0.90 ± 0.04	1.73 ± 0.45	8.72 ± 1.83	4.03 ± 0.12
20,000 g pellet (3)	5.15 ± 2.19	1.11 ± 0.30	20.00 ± 5.94	14.73 ± 0.96
160,000 g pellet (4)	3.27 ± 1.20	5.54 ± 1.41	8.43 ± 1.29	3.67 ± 0.34

Similar insects also were treated with AKH, respectively. Distribution of total radioactivity among subcellular fractions is expressed as a percentage of total counts per min ± SEM of n experiments. Total counts per min represents the counts per min that were recovered from all the fractions after the subcellular fractionation for each case separately. Values of total counts per min were as follows: $6.1 (\pm 0.3) \times 10^6$, $5.8 (\pm 0.2) \times 10^6$, $8.2 (\pm 2.4) \times 10^6$, and $5.8 (\pm 0.9) \times 10^6$ for long term, long term/AKH, short term, short term/AKH, respectively.

TABLE 4. Distribution of radioactive DG among subcellular fractions from insects that were short-term or long-term radiolabeled with [³H]palmitic acid.

Subcellular Fraction	Diacylglycerols (%)			
	Long Term		Short Term	
	-AKH (n = 3)	+AKH (n = 4)	-AKH (n = 4)	+AKH (n = 3)
Fat cake (1)	2.00 ± 0.17 (62.3%)	4.86 ± 0.35 (88.9%)	1 2.5 ± 1.65 (57.9%)	7.20 ± 0.17 (70.4%)
Cytosol (2)	0.092 ± 0.002 (2.9%) ^a	0.3 ± 0.06 (5.7%) ^c	2.04 ± 0.69 (9.4%) ^b	0.49 ± 0.08 (4.8%) ^d
20,000 g pellet (3)	0.57 ± 0.01 (17.8%)	0.40 ± 0.09 (7.3%)	4.70 ± 1.00 (21.7%)	2.05 ± 0.20 (20.0%)
160,000 g pellet (4)	0.52 ± 0.11 (16.2%)	0.25 ± 0.06 (4.6%)	2.36 ± 0.65 (9.6%)	0.49 ± 0.17 (4.8%)
Σ % DG in fractions 1-4	3.21 ± 0.12	5.47 ± 0.07	21.61 ± 2.76	10.23 ± 0.36
% DG in whole homogenate ^e	3.25 ± 0.27	5.11 ± 0.32	22.10 ± 3.50	10.80 ± 0.18

Similar insects also were treated with AKH, respectively. Radioactivity in DG is expressed as a percentage of total counts per min. Total counts per min represents the sum of counts per min that were recovered in each subcellular fraction as indicated in the legend to Table 3. Values represent means ± SEM of n experiments.

^{a,b} P = 0.0161.

^{c,d} P = NS.

^e These values were determined in aliquots of fat body homogenate previous to the subcellular fractionation.

Ficoll fractionation

To leave the cell, DG might first have to accumulate in the plasma membrane; therefore, it was of interest to investigate the presence of radioactive DG in the plasma membrane. Plasma membranes were separated from the mitochondrial fraction by means of a Ficoll gradient as indicated in Materials and Methods. Again, the distribution of total radioactivity and the lipid composition of each fraction were determined (data not shown). **Table 5** shows the distribution of radioactive DG and total protein between the two Ficoll fractions: top (T), which corresponds to the plasma membrane and bottom (B), which corresponds to the mitochondrial fraction. As can be seen, activation of lipolysis did not alter the proportion of either bulk or newly DG located in the plasma membrane (Table 5). This result shows that the intracellular transport and secretion of DG did not involve an accumulation of DG in the plasma membrane.

Unlike the proportion of DG in the plasma membrane, the activation of lipolysis affected the DG located in the mitochondrial fraction. Both bulk and newly synthesized DG exhibited a 9-fold decrease after hormonal treatment. At this time, we do not have an explanation for this result. However, the fact that both mitochondrial pools of DG

were similarly affected by the activation of lipolysis could be an indication that the origin of the bulk DG is the same as the origin of newly synthesized DG. Consequently, bulk DG present in the mitochondria could be (re)esterified FFA that were taken from the hemolymph.

Density fractionation of the cytosol

KBr gradients were performed in order to investigate whether the cytosolic lipids were associated with some type of low density structure or particle. **Table 6** shows the distribution of cytosolic DG among the four density gradient fractions. An almost even distribution of DG along the gradient was found, whereas a 5-fold increase in the protein concentration from the top toward the bottom of the gradient was detected. The presence of DG at the top of the gradient suggests that some DG-rich particles could be present in the cytosolic fraction.

Apparent specific activities of newly synthesized DG in the subcellular fractions

As mentioned above, the fact that the distribution of radioactivity in long-term prelabeling coincides with the distribution of the mass allows us to estimate an apparent specific activity of newly synthesized DG. For this purpose,

TABLE 5. Distribution of radioactive DG among subcellular fractions from insects that were short-term or long-term radiolabeled with [³H]palmitic acid

Ficoll Fractionation	Diacylglycerols (%)			
	Long Term		Short Term	
	-AKH (n = 3)	+AKH (n = 4)	-AKH (n = 4)	+AKH (n = 3)
Top (T): 0.39 ± 0.01 mg protein/insect ^a	0.45 ± 0.05	0.44 ± 0.09	1.08 ± 0.26	1.24 ± 0.11
Bottom (B): 1.63 ± 0.09 mg protein/insect ^a	0.43 ± 0.07	0.05 ± 0.01	2.55 ± 0.35	0.26 ± 0.04
Σ % DG in fractions T + B	0.88 ± 0.11	0.49 ± 0.09	3.63 ± 0.44	1.50 ± 0.15
% DG in lowspeed pellet ^b	0.57 ± 0.01	0.40 ± 0.09	4.70 ± 1.00	2.05 ± 0.20

Similar insects were also treated with AKH, respectively. Radioactivity in DG is expressed as a percentage of total counts per min. Total counts per min represents the sum of counts per min that was recovered in each subcellular fraction as indicated above. Values represent means ± SEM of n experiments.

^a Total protein (mg) per insect.

^b These values were determined in aliquots of 20,000 g pellets before the Ficoll gradient.

TABLE 6. Distribution of radioactive DG found in the cytosol among the density gradient fractions from insects that were short-term or long-term radiolabeled with [³H]palmitic acid

Fraction	KBr Fractionation Density (g/ml)/Total Protein (mg/insect)	Diacylglycerols (%)			
		Long Term		Short Term	
		-AKH (n = 3)	+AKH (n = 4)	-AKH (n = 4)	+AKH (n = 3)
a	1.096 ± 0.005/1.47 ± 0.09	0.026 ± 0.002	0.100 ± 0.050	0.23 ± 0.07	0.110 ± 0.020
b	1.121 ± 0.003/2.92 ± 0.16	0.037 ± 0.007	0.102 ± 0.030	0.52 ± 0.17	0.177 ± 0.024
c	1.153 ± 0.006/4.57 ± 0.27	0.023 ± 0.007	0.093 ± 0.030	0.58 ± 0.16	0.200 ± 0.026
d	1.189 ± 0.005/7.35 ± 0.52	0.041 ± 0.005	0.099 ± 0.031	0.43 ± 0.07	0.170 ± 0.033
Σ % DG in fractions a–d		0.127 ± 0.010	0.380 ± 0.120	1.50 ± 0.13	0.660 ± 0.080
% DG in cytosol ^a		0.092 ± 0.02	0.310 ± 0.060	2.04 ± 0.69	0.490 ± 0.080

Similar insects also were treated with AKH, respectively. Radioactivity in DG is expressed as a percentage of total counts per min. Total counts per min represents the sum of counts per min that was recovered in each subcellular fraction as indicated above. Values represent means ± SEM of n experiments.

^a These values were determined in aliquots of cytosol previous to the KBr gradient.

and for each subcellular fraction, we obtained the ratio of the percent radioactivity found in short-term labeled DG to the corresponding value of percent radioactivity found in long-term labeled DG (Table 3).

Figure 3A shows calculations that were done in the absence and presence of AKH. The fat cake and, particularly, the cytosolic fraction were the two subcellular fractions in which a significant change of DG-apparent specific activity was observed after the hormonal stimulation of lipolysis.

The apparent specific activity of the two Ficoll fractions is shown in Fig. 3B. No significant change in the DG-apparent specific activity between the absence and presence of AKH was observed in the plasma membrane or mitochondrial fraction. As mentioned before, the activation of lipolysis promoted a decrease in the DG contained in the mitochondria. However, given the fact that bulk and newly synthesized DG decreased by the same extent, the apparent specific activity of this fraction remained unchanged (Fig. 3B). Figure 3C shows the apparent specific activity of DG in the four density fractions after the KBr fractionation of the cytosol. Large changes in DG-apparent specific activity were observed in all the KBr fractions, although the changes in fractions a and d were the most statistically significant.

DISCUSSION

Lipid mobilization induced by injection of AKH into resting insect resulted in a dramatic elevation of DG in hemolymph (5). One hour after the injection of AKH, the DG content of the hemolymph increased nearly 2-fold, from 12 to 21 mg, at the expense of fat body TG. The intracellular content DG in the fat body also increased from 1.7 to about 2.9 mg per fat body. However, the smaller amount of DG accumulated in the fat body, compared with the amount of secreted DG, clearly indicates that the fat body cell is actively producing and, simultaneously, exporting DG to the hemolymph. This machinery of DG production and secretion constitutes a unique system with

which to study the intracellular mechanisms of transport and secretion of DG.

DG represents less than 3% of the lipid mass of the fat body. However, 20% of the FA that enter the fat body are rapidly converted into DG. The large fraction of FA converted into DG is obtained with any of the two more abundant FA, palmitic and oleic acid, of the insect. This disproportion between new and bulk DG indicates that newly synthesized DG does not equilibrate rapidly with the bulk lipids and constitutes a different pool. This is the first report showing this accumulation of DG in insect cells. Interestingly, a similar situation for newly synthesized DG was found in adipose tissue from vertebrates, where accumulation between 20% and 50% has been reported (22–25). This is particularly interesting because these two tissues mobilize lipids via different pathways. Even though the secretion of DG has not been shown in vertebrates, the fact that cells from both vertebrate and invertebrate fat tissues accumulate newly synthesized DG points out that this phenomenon is a common aspect of lipid biosynthesis. It is also interesting to note that in both systems the newly synthesized DG pool has a relatively long half-life; the proportion of this pool remained quite constant for at least 5 h in the fat body (Fig. 1A and B). Thus, newly synthesized DG must somehow remain inaccessible to the TG biosynthetic pathway for several hours.

The mechanism that prevents equilibration of the newly synthesized DGsl with the bulk DG is unknown.

Stimulation of lipolysis by AKH produces a fast decrease in the fraction of short-term radiolabeled DG, whereas, concomitantly, there is an increase in the mass of fat-body DG (Fig. 2 and text). This fact indicates that recently synthesized DG are preferentially mobilized and secreted, constituting part of a highly dynamic lipid pool.

Most of the bulk DG (62.3%) was found in the fat cake: 34% was distributed among mitochondria, plasma membrane, and microsomes; whereas only 2.9% was found in the cytosol (Table 4). When lipolysis was stimulated, the fat cake and cytosol were the fractions that had the highest accumulation of DG (Table 4).

The majority (57.9%) of the newly synthesized DG was

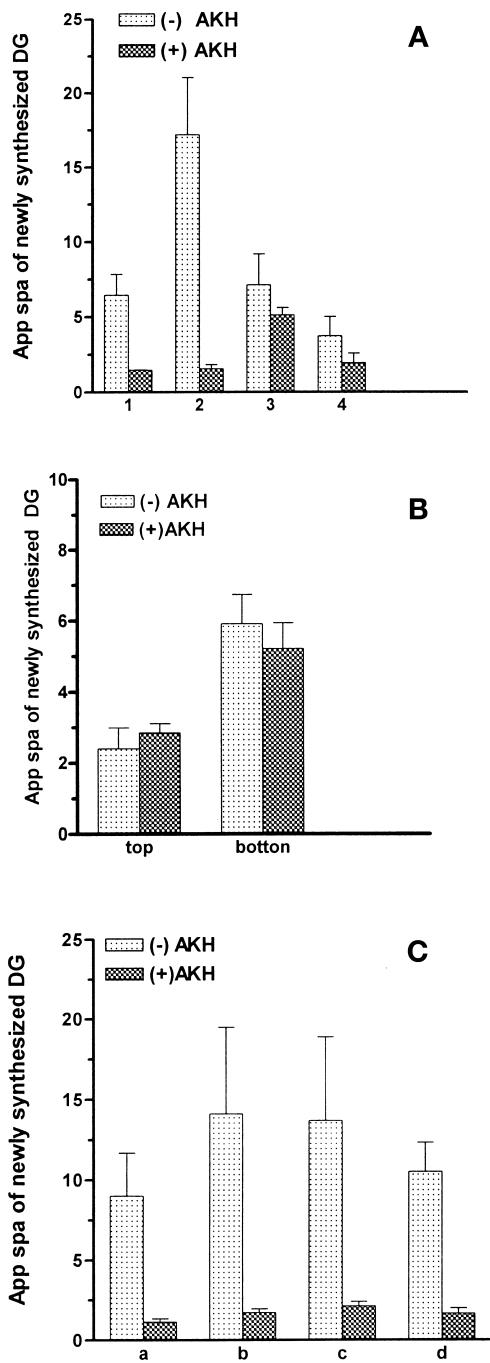


Fig. 3. Apparent specific activities (App spa) of newly synthesized DG in the subcellular fractions before and after treatment with AKH. Apparent specific activity was calculated by dividing the proportion of DG obtained in the short-term labeling by the corresponding value obtained in the long-term labeling. A: Fat cake (1), cytosol (2), 20,000 g pellet (3), and 160,000 g pellet (4). B: Ficoll fractions: plasma membrane fraction (top) and mitochondrial fraction (bottom) as described in Table 6. C: KBr fractions of the cytosol: a, b, c, and d fractions as described in Table 6.

also found in the fat cake, but a larger part (9.4%) was present in the cytosolic fraction (Table 4). This subcellular distribution seems to be consistent with the fact that DG to be secreted must be segregated from the last step of the TG biosynthetic pathway, in which the microsomal

diacylglycerol-acyltransferase catalyzes the acylation of DG to form TG (26). After hormonal stimulation of lipolysis, a significant decrease in the apparent specific activity of newly synthesized DG was observed only in the fat cake and the cytosolic fractions, with the biggest decrease occurring in the cytosolic fraction (Fig. 3). These results suggest that the newly synthesized DG present in the fat cake and the cytosol are the direct precursors of exported DG. These results also indicate that bulk TG in the fat cake is the major source of exported DG.

Because long-chain DGs are highly insoluble in the aqueous media, they must be associated with other components in the cytosol such as proteins and/or phospholipids. In this regard, one report suggests that intracellular stabilization of DG in a vertebrate system could occur in a micellar form similar to the lipoprotein, lipophorin, present in the insect hemolymph (27). That report showed that *in vitro* incubation of rat liver cytosol with DG resulted in the formation of stable DG-protein complexes characterized as micelles according to the elution pattern in gel-filtration chromatography (27). We found either bulk or newly synthesized DGs distributed almost evenly in all the fractions, after density gradient fractionation of the cytosol (Table 6). However, a significant increase in the proportion of DG expressed per milligram of protein was observed as the density of the fractions decreased. The occurrence of particles with increasing content of DG and concomitantly decreasing densities could explain this observation. Further experiments are necessary to clarify this observation.

The intracellular transport of DG is an aspect of lipid mobilization in insects that remains to be elucidated. In view of these results, it would appear that this process involves two steps: first, TG would be converted into DG catalyzed by the TG lipase on the surface of the lipid storage droplet; afterward, DG would be transferred to a cytosolic carrier, which in turn would target the delivery of DG across the plasma membrane. Our results indicate that the intracellular transport and secretion of DG did not involve an accumulation of DG in the plasma membrane. The cytosolic carrier could be a specialized protein that binds DG, with properties similar to the adipocyte FA-binding protein (A-FABP), which has been described as a "membrane-interactive protein" because it interacts with phospholipid bilayers (28). Likewise, it has been proposed that A-FABP facilitate the intracellular trafficking of hydrophobic lipids (29). Confirmation of the proposed mechanism requires the isolation of the carrier. We conclude that the newly synthesized DG could be used for studying the transport of DG within the cell and it could facilitate the search for the putative carrier. **□**

We thank Mary Hernandez for animal care. This work was supported by National Institutes of Health grant GM 51296 to M.A.W, GM 55622 to J.L.S., and the Oklahoma Agricultural Experimental Station. The Undergraduate Biology Research Program of the University of Arizona supported M.T.F. and J.L.G.

Manuscript received 1 July 2000 and in revised form 9 October 2000.

REFERENCES

1. Beenackers, A. M. T., D. J. Van der Host, and W. J. A. Van Marrewijk. 1985. Insect lipids and lipoproteins and their role in physiological processes. *Prog. Lipid Res.* **24**: 9–67.
2. Arrese, E. L., and M. A. Wells. 1997. Adipokinetic hormone-induced lipolysis in the fat body of an insect, *Manduca sexta*: synthesis of *sn*-1,2-diacylglycerols. *J. Lipid Res.* **38**: 68–76.
3. Orchard, I. 1987. Adipokinetic hormone: an update. *J. Insect Physiol.* **161**: 125–131.
4. Arrese, E. L., M. T. Flowers, J. L. Gazard, and M. A. Wells. 1999. Calcium and cAMP are second messengers in the adipokinetic hormone-induced lipolysis of triacylglycerols in *Manduca sexta* fat body. *J. Lipid Res.* **40**: 556–564.
5. Arrese, E. L., B. I. Rojas-Rivas, and M. A. Wells. 1996. The use of decapitated insects to study lipid mobilization in adult *Manduca sexta*: effects of adipokinetic hormone and trehalose on fat body lipase activity. *Insect Biochem. Mol. Biol.* **26**: 775–782.
6. Holm, C., T. Østerlund, H. Laurell, and J. A. Contreras. 2000. Molecular mechanisms regulating hormone-sensitive lipase and lipolysis. *Annu. Rev. Nutr.* **20**: 365–393.
7. Gibbons, G. F., K. Islam, and R. J. Pease. 2000. Mobilisation of triacylglycerol stores. *Biochim. Biophys. Acta.* **1438**: 37–57.
8. Morimoto, C., M. Sumiyoshi, K. Kameda, T. Tsujita, and H. Okuda. 1999. Relationship between hormone-sensitive lipolysis and lipase activity in rat fat cells. *J. Biochem.* **125**: 976–981.
9. Morimoto, C., T. Tsujita, M. Sumida, and H. Okuda. 2000. Substrate-dependent lipolysis induced by isoproterenol. *Biochem. Biophys. Res. Commun.* **274**: 631–634.
10. Arrese, E. L., B. I. Rojas-Rivas, and M. A. Wells. 1996a. Synthesis of *sn*-1,2-diacylglycerols by monoacylglycerol-acyltransferase from *Manduca sexta* fat body. *Arch. Insect Biochem. Physiol.* **31**: 325–335.
11. Soulages, J. L., and M. A. Wells. 1994. Lipophorin: the structure of an insect lipoprotein and its role in lipid transport in insects. *Adv. Protein Chem.* **45**: 371–415.
12. Downer, R. G. H., and H. Chino. 1985. Turnover of protein and diacylglycerol components of lipophorin in insect hemolymph. *Insect Biochem.* **15**: 627–630.
13. Van Heusen, M. C., and J. H. Law. 1989. An insect lipid transfer particle promotes lipid loading from fat body to lipoprotein. *J. Biol. Chem.* **264**: 17287–17292.
14. Willot, E., L. K. Bew, R. B. Nagle, and M. A. Wells. 1988. Sequential structural changes in the fat body of the tobacco hornworm, *Manduca sexta*, during the fifth larval stadium. *Tissue Cell.* **20**: 635–643.
15. Arrese, E. L., and M. A. Wells. 1994. Purification and properties of the phosphorylatable triacylglycerol-lipase from the fat body of an insect, *Manduca sexta*. *J. Lipid Res.* **35**: 1652–1659.
16. Ziegler, R. 1991. Changes in lipid and carbohydrate metabolism during starvation in adult *Manduca sexta*. *J. Comp. Physiol. B.* **161**: 125–131.
17. Folch, J., M. Lees, and G. H. Sloane Stanley. 1957. A simple method for isolation and purification of total lipids from animal tissues. *J. Biol. Chem.* **226**: 497–509.
18. Skispi, V. P., and N. Barclay. 1969. Thin-layer chromatography of lipids. *Methods Enzymol.* **14**: 530–611.
19. Brockman, H. 1981. Triglyceride lipase from porcine pancreas. *Methods Enzymol.* **71**: 619–627.
20. Jarret, L. 1974. Subcellular fractionation of adipocytes. *Methods Enzymol.* **31**: 60–71.
21. Bradford, M. M. 1976. A rapid and sensitive method for the quantitation of microgram quantities of protein utilizing the principle of protein-dye binding. *Anal. Biochem.* **72**: 248–254.
22. Angel, A. 1970. Studies on the compartmentation of lipid in adipose cells. I. Subcellular distribution, composition, and transport of newly synthesized lipid: liposomes. *J. Lipid Res.* **11**: 420–432.
23. Zinder, O., E. Eisenberg, and B. Shapiro. 1973. Compartmentation of glycerides in adipose tissue cells. I. The mechanism of free fatty acid release. *J. Biol. Chem.* **248**: 7673–7676.
24. Winand, J., J. Furnelle, C. Wodon, and J. Christophe. 1971. Spectrum of fatty acids synthesized in situ and metabolic heterogeneity of free fatty acids and glycerides within isolated rat adipocytes. *Biochim. Biophys. Acta.* **239**: E140–E147.
25. Edens, N. K., R. L. Leibel, and J. Hirsch. 1990. Lipolytic effects on diacylglycerols accumulation in human adipose tissue in vitro. *J. Lipid Res.* **31**: 1351–1359.
26. Bell, R. M., L. M. Ballas, and R. A. Coleman. 1981. Lipid topogenesis. *J. Lipid Res.* **22**: 391–403.
27. Florin-Christensen, J., C. D'Alessio, C. Arighi, J. Caramelo, M. Florin-Christensen, and J. M. Delfino. 1998. Micellar lipoproteins as the possible storage and translocation form of intracellular diacylglycerol. *Biochem. Biophys. Res. Commun.* **243**: 669–673.
28. Gericke, A., E. R. Smith, D. J. Moore, R. Mendelsohn, and J. Stoch. 1997. Adipocyte FA-binding protein: interaction with phospholipid membranes and thermal stability by FTIR spectroscopy. *Biochemistry.* **36**: 8311–8317.
29. Shen, W., K. Sridhar, D. A. Bernlohr, and F. B. Kraemer. 1999. Interaction of rat-hormone-sensitive-lipase with adipocyte lipid-binding protein. *Proc. Natl. Acad. Sci. USA.* **96**: 5528–5532.